NASA Technical Memorandum 103906

A Rotorcraft Flight Database for Validation of Vision-Based Ranging Algorithms

Phillip N. Smith, Ames Research Center, Moffett Field, California

April 1992

National Aeronautics and
Space Administration

Ames Research Center
Moffett Field, California 94035-1000

SUMMARY

Computer vision research has led to the development of several algorithms for estimating range to obstacles during low-altitude flight. However, due to the limited availability of "real world" data, algorithm verification has not been effectively addressed. A helicopter flight test experiment has been conducted at NASA Ames Research Center to obtain a database consisting of video imagery and accurate measurements of camera motion, camera calibration parameters, and true range information. The database was developed to allow verification of monocular passive range estimation algorithms for use in the autonomous navigation of rotorcraft during low altitude flight. This paper briefly describes the helicopter flight experiment and presents four data sets representative of the different helicopter maneuvers and the visual scenery encountered during the flight test. These data sets will be made available to researchers in the computer vision community.

INTRODUCTION

NASA, in conjunction with the US Army, has been pursuing research in autonomous navigation of rotorcraft during low-altitude flight in order to reduce the high pilot workload associated with obstacle avoidance (ref. 1). In one approach, obstacle information is acquired by a computer vision system located on board the rotorcraft. The obstacle information would be used to generate advisory displays and serve as an input to an automatic guidance system capable of performing the obstacle avoidance task autonomously. Research at Ames (refs. 2-4) has focused on the development of range estimation algorithms and obstacle avoidance algorithms for autonomous navigation (ref. 5). Since military helicopters are increasingly being equipped with inertial systems to measure the vehicle's motion states for guidance and stability augmentation systems, the range estimation algorithms use knowledge of the camera's motion (position, orientation, linear velocity, and angular velocity) and estimate the range to environmental points.

Experimental data are needed to establish the validity of algorithms and to investigate factors encountered in real world data that affect algorithmic performance. A laboratory facility has been developed at Ames to provide the first stage of algorithm verification (ref. 6). Further development and testing of these algorithms require data collected from rotorcraft flight. Current databases available in the literature contain some motion information and true range measurements for outdoor scenery (refs. 7-9) but they either do not provide extensive motion measurements or they do not describe the general camera motion (translation and rotation) encountered in flight. A flight experiment has been conducted to obtain the video imagery, camera motion, camera calibration parameters, and true range information for testing algorithms with realistic data. It is hoped that availability of these data sets will facilitate the comparison of different motion analysis methods.

DATA SET DEVELOPMENT

Figure 1 depicts the flight experiment designed to acquire the necessary measurements of rotorcraft motion states, video imagery, and true range information. A Cohu 6410-series monochrome CCD video camera was mounted rigidly under the nose of a CH-47B Chinook helicopter and oriented approximately along the longitudinal body axis to observe obstacles that the rotorcraft would encounter in forward

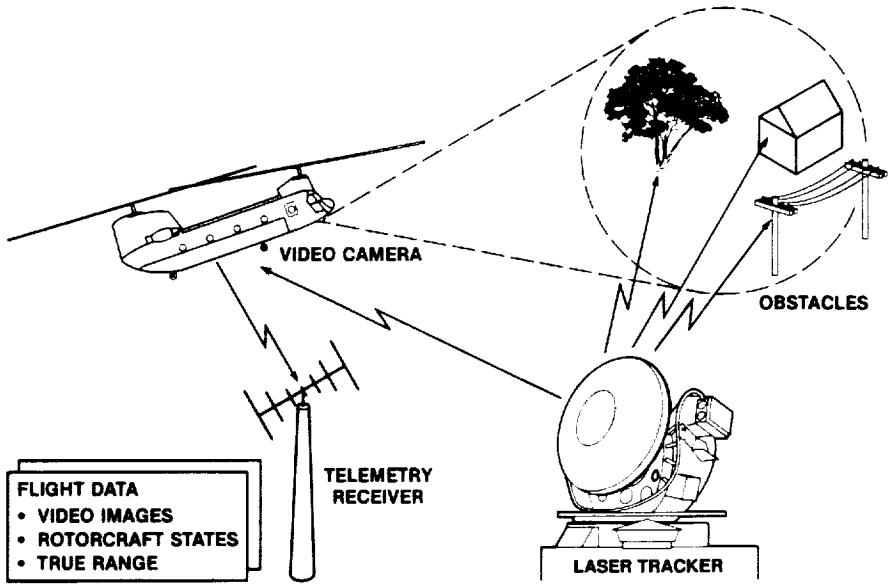

Figure 1. Flight experiment overview.

flight. The camera produces standard RS-170 interlaced video output and has an electronic shutter which was set for 1 msec exposure time (per video field). The analog video signal was recorded by a U-matic video tape recorder located onboard the CH-47.

The rotorcraft motion states were measured by instrumentation on board the CH-47, filtered, digitized, and transmitted to a ground station facility for recording. Raw measurements including linear accelerations, Euler angles, and angular rates were collected. The instruments were aligned with the helicopter's body axes which originate at the helicopter's center of gravity. The body axes system and other coordinate systems of interest are illustrated in figure 2. Derivation of the camera motion states from the measured rotorcraft motion states requires knowledge of the position and orientation of the camera axes system relative to the helicopter body axes system, as will be addressed later in this section. The motion measurements have a minimum bandwidth of 10 Hz and were sampled at approximately 110 Hz. The rotational frequency of the helicopter's rotor blades is about 11 Hz.

True range measurements were obtained by a two-step process using a laser tracker. First, the laser tracker measured the position in Earth axes of a rotorcraft-mounted reflector throughout each test flight, and the resulting data (also at 110 Hz) were recorded at the ground station on a common time base with the telemetry data. Second, at the completion of a test flight, the laser tracker was used to measure the position in Earth axes of the (stationary) objects that served as the obstacles of interest. A laser reflector was manually placed at each obstacle location to obtain the position information.

To coordinate the imagery data with the rotorcraft state data and the true range measurements, a time source onboard the CH-47 was synchronized with the time source at the ground station to 1-msec accuracy. A message containing the current time was then displayed in the upper left-hand corner of each video image.

Significant post-flight processing of the data was required to develop the raw measurements into a final form suitable for motion analysis research. An overview of the post-flight processing procedure is

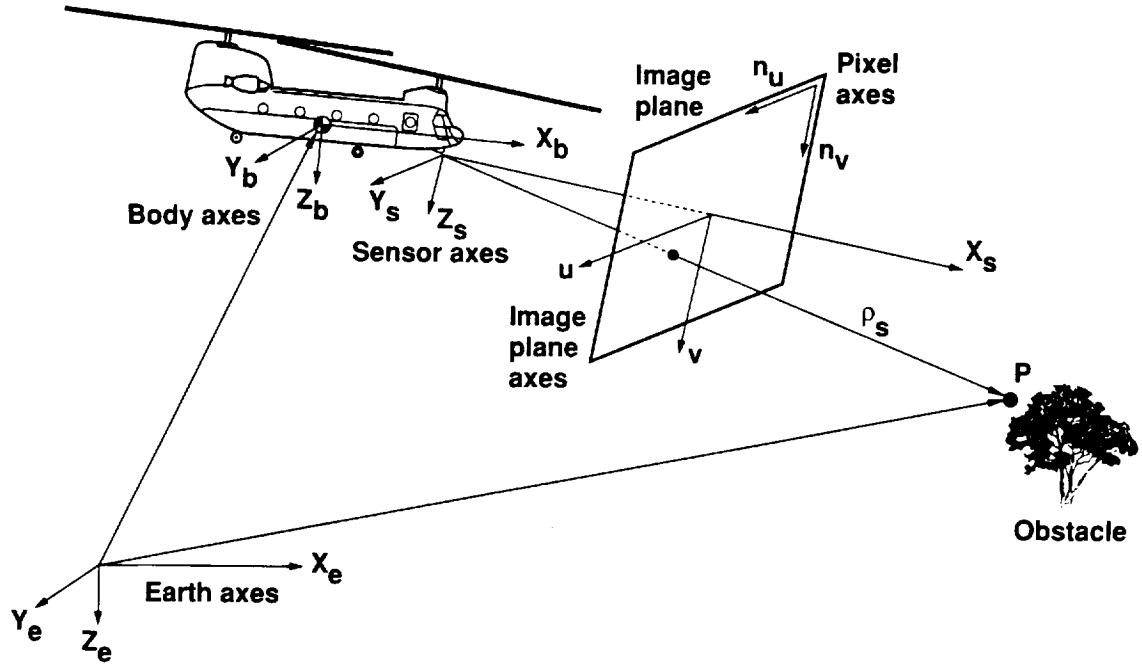

Figure 2. Flight experiment geometry.

shown in figure 3. Helicopter motion measurements were corrected to the CG-centered body axes using instrument position information. The location in body axes of the laser reflector was used along with helicopter orientation information to determine the helicopter CG location in Earth axes from the raw laser measurements. All measurements were then low-pass filtered at 10 Hz before eventual subsampling to 30 Hz video rate.

The motion states were processed using a state estimation algorithm (ref. 10) to check the accuracy and kinematic consistency of the measurements. This algorithm uses the well-known rigid body kinematic equations of motion to process the measurements in an "optimal" way to ensure internal consistency of measured states, improve knowledge of poorly measured states, identify instrument bias and scale factor errors, and estimate states during periods of telemetry dropout. Since direct measurements of linear velocity were unavailable, velocity information was reconstructed by state estimation based upon position and acceleration measurements. The end result is a single best estimate of the rotorcraft motion states (position, orientation, linear velocity, angular rates, and linear accelerations) based on all available measurements. The motion states are consistent with instrument accuracy for frequencies up to 15 Hz. State estimation processing was used to develop a high-precision, internally consistent data set for research purposes; however, for operational systems the state measurement information required for passive range estimation would be acquired directly from onboard instrumentation.

Knowledge of the position and orientation of the camera axes system with respect to the helicopter body axes system is necessary to derive the camera motion states (in camera axes) given the rotorcraft motion states (in body axes). The camera axes originate at the camera lens focal point with the X_s axis oriented along the optical axis and the Y_s and Z_s axes oriented along the rows and columns, respectively, of the sensor array (see fig. 2). The position and orientation of the camera axes are known as the external camera calibration parameters. Additional information about the camera such as the focal length, the location of the image center (where the optical axis passes through the image plane),

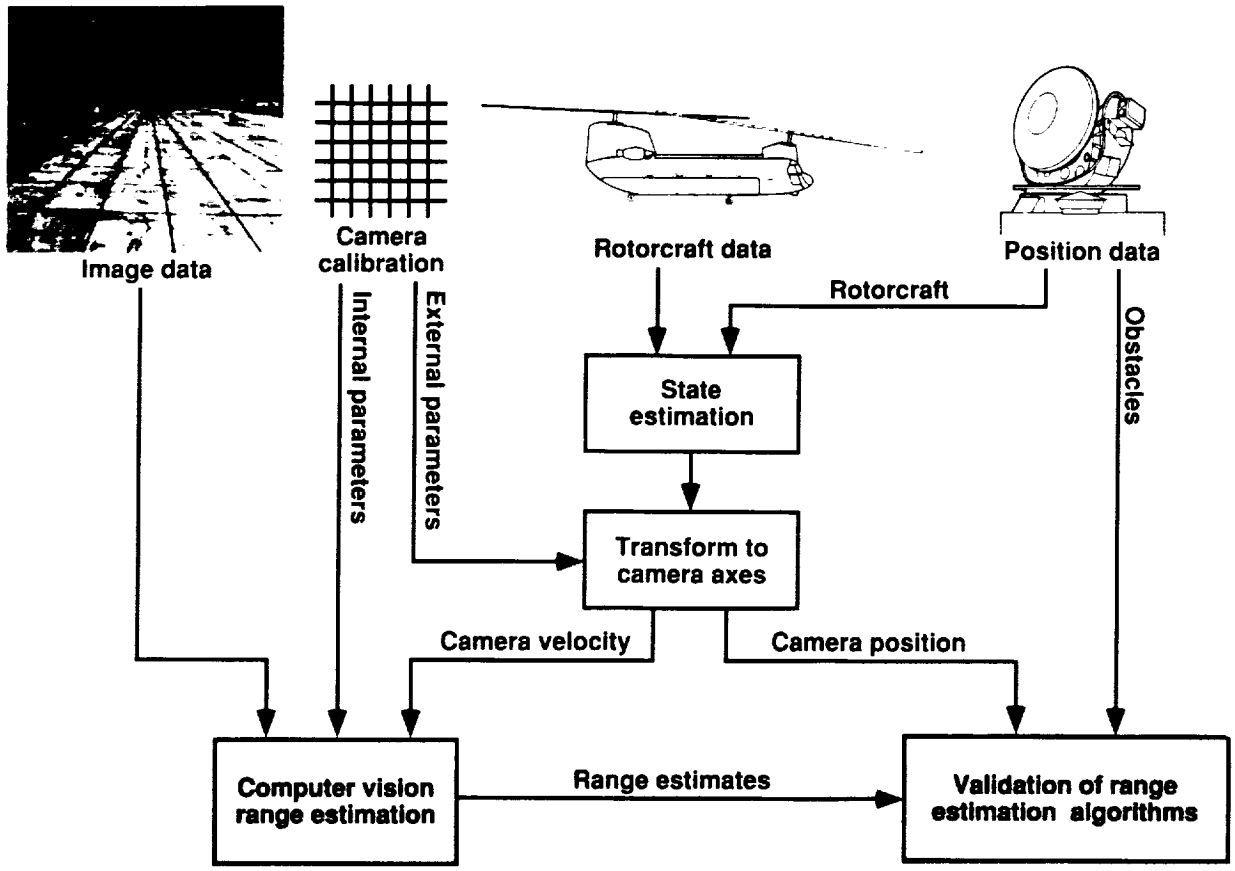

Figure 3. Development of data set elements.

and the effective pixel aspect ratio (known collectively as the internal camera calibration parameters) is also necessary for motion analysis.

It is difficult to directly measure even the external parameters with sufficient accuracy, so both the internal and external parameters are determined experimentally. The external parameters map points from body axes to camera axes and the internal parameters map points from camera axes to locations on the image plane. By measuring the location of points in body axes and the corresponding pixel location where the points appears in an image, it is possible to estimate the internal and external parameters. While conceptually straightforward, the measurement in body axes of points in the camera's field of view is a challenging experimental task. The method used to collect the experimental data and the technique developed to estimate the unknown parameters are discussed in reference 11.

DATA SET CONTENTS

The flight experiment and processing of the raw data results in the following information:

1. digitized imagery (30 frames/sec)
2. sensor velocity and angular rates in camera axes
3. sensor position and orientation in Earth axes

4. rotorcraft velocity and angular rates in body axes
5. rotorcraft position and orientation in Earth axes
6. internal camera calibration parameters
7. external camera calibration parameters
8. obstacle positions in Earth axes

The digitized images are 512 × 512 pixels with 256 gray levels. The rotorcraft and camera motion measurements corresponding to each image as well as the camera calibration parameters are stored in a header that prefaces each image. Specific remarks concerning use of the image header contents may be found in the appendix. The obstacle position measurements in Earth axes are provided in a separate file. Each image header contains the information necessary to express obstacle positions in terms of the helicopter body axes, camera axes, or image plane pixel coordinates. Figures 4-7 show sample images collected during the flight experiment. The object visible in the upper right-hand corner of each image is the helicopter's nose boom. The motion and calibration information for the left-hand image in figure 4 is given in table 1. The image header contains the data in the first two columns of the table. The information concerning accuracy and units is the same for all image headers. Table 2 contains the position measurements in Earth axes for the labelled points in figures 4 and 5.

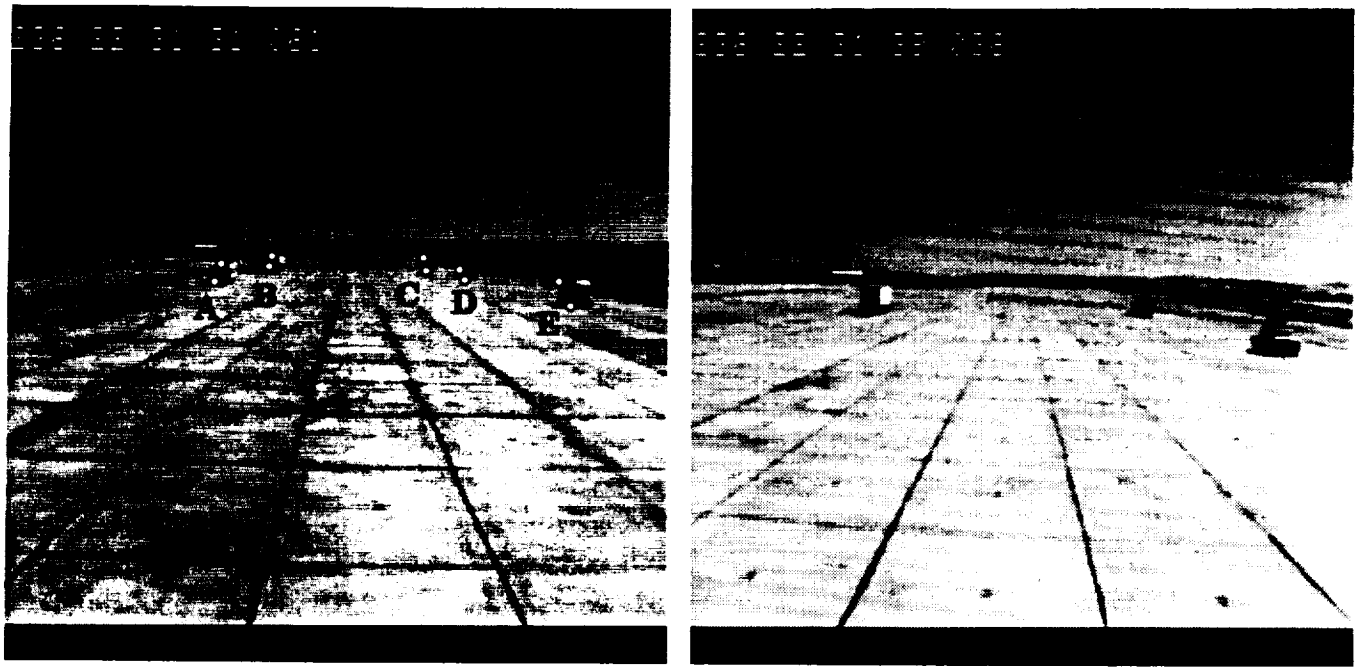

Figure 4. First and last images of Line data set.

Table 1. Sample image header data

Measurement name	Value	Accuracy	Units
SENSOR_POSITION_X_WORLD	734		feet
SENSOR_POSITION_Y_WORLD	520		feet
SENSOR_POSITION_Z_WORLD	−11		feet
BODY_POSITION_X_WORLD	757	2.0	feet
BODY_POSITION_Y_WORLD	517	2.0	feet
BODY_POSITION_Z_WORLD	−16	2.0	feet
SENSOR_VELOCITY_X_SENSOR	30.2		feet/sec
SENSOR_VELOCITY_Y_SENSOR	0.2		feet/sec
SENSOR_VELOCITY_Z_SENSOR	−1.9		feet/sec
SENSOR_ANGULAR_RATE_X_SENSOR	0.0238		rad/sec
SENSOR_ANGULAR_RATE_Y_SENSOR	0.0113		rad/sec
SENSOR_ANGULAR_RATE_Z_SENSOR	0.0124		rad/sec
BODY_VELOCITY_X_BODY	30.1	0.3	feet/sec
BODY_VELOCITY_Y_BODY	0.1	0.3	feet/sec
BODY_VELOCITY_Z_BODY	2.6	0.6	feet/sec
BODY_ANGULAR_RATE_X_BODY	0.0218	0.0045	rad/sec
BODY_ANGULAR_RATE_Y_BODY	0.0115	0.0045	rad/sec
BODY_ANGULAR_RATE_Z_BODY	0.0155	0.0025	rad/sec
SENSOR_POSITION_X_BODY	22.950	0.042	feet
SENSOR_POSITION_Y_BODY	−1.043	0.017	feet
SENSOR_POSITION_Z_BODY	6.940	0.017	feet
ANGLE_PSI_WORLD_TO_BODY	3.0348	0.0123	radians
ANGLE_THETA_WORLD_TO_BODY	0.0646	0.0021	radians
ANGLE_PHI_WORLD_TO_BODY	−0.0153	0.0042	radians
ANGLE_PSI_BODY_TO_SENSOR	0.0055	0.0035	radians
ANGLE_THETA_BODY_TO_SENSOR	−0.1393	0.0035	radians
ANGLE_PHI_BODY_TO_SENSOR	−0.0074	0.0017	radians
ANGLE_PSI_WORLD_TO_SENSOR	3.0424		radians
ANGLE_THETA_WORLD_TO_SENSOR	−0.0746		radians
ANGLE_PHI_WORLD_TO_SENSOR	−0.0223		radians
ASPECT_RATIO	1.005	0.001	non-dimensional
FOCAL_LENGTH	621.4	2.6	pixels
U_CENTER	253.3	2.4	pixels
V_CENTER	238.3	1.6	pixels
STAMP_TIME	236:22:31:31.061		seconds
GLOBAL_TIME	81091.061		seconds
DELTA_TIME	0.033		seconds
FRAMEID	0		non-dimensional

Table 2. Sample true obstacle position data

Label	Obstacle name	X_e, ft	Y_e, ft	Z_e, ft
A	truck 2, NE ground level	368.7 ± 2	614.1 ± 2	4.5 ± 2
B	truck 2, SE top corner	348.7	614.5	–3.1
C	truck 4, NE ground level	118.3	633.1	3.6
D	truck 4, SE top corner	98.6	634.8	–7.4
E	truck 5, NE ground level	–17.7	510.6	3.0
F	truck 5, SE top corner	–37.6	511.5	–7.7
G	truck 3, NE ground level	231.2	490.2	3.9
H	truck 3, SE top corner	209.0	491.9	–0.2
I	truck 1, NE ground level	479.3	470.6	4.9
J	truck 1, SE top corner	461.5	472.3	–3.0
K	truck 1, mast tip	460.0	466.7	–24.3

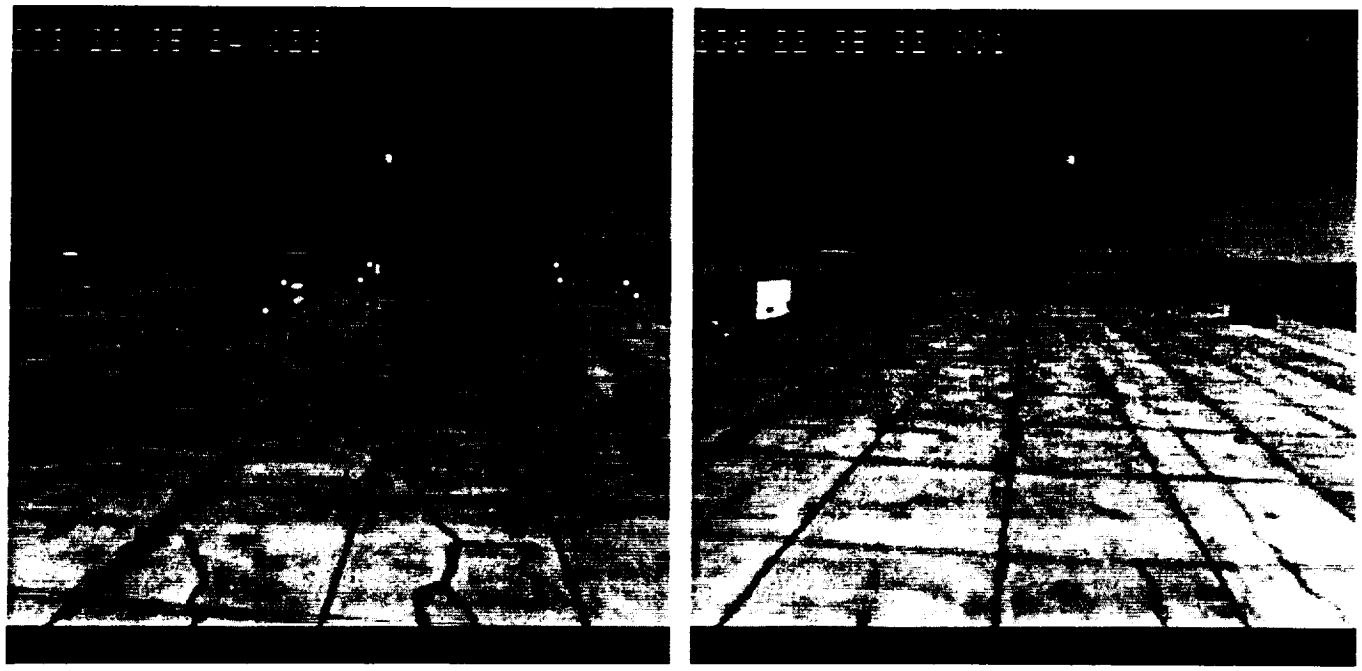

Figure 5. First and last images of Arc data set.

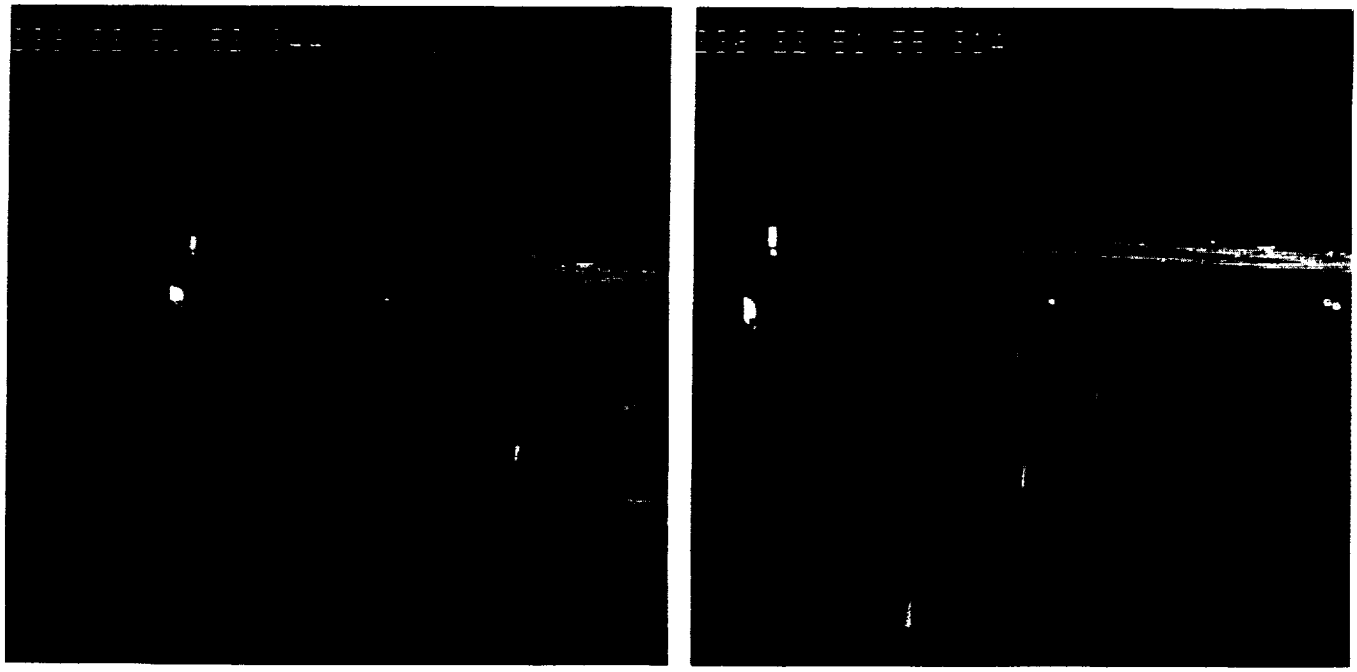

Figure 6. First and last images of Posts data set.

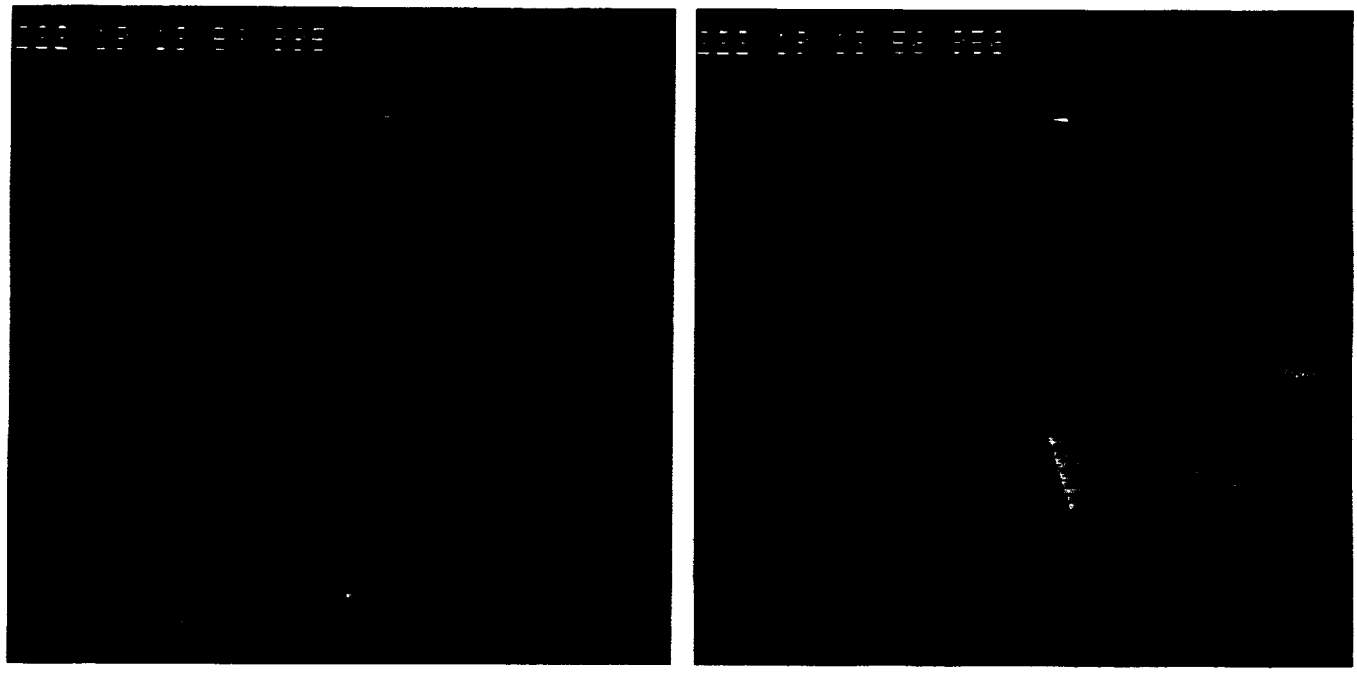

Figure 7. First and last images of Towers data set.

EXAMPLE DATA SETS

Each of the following data sets was selected to demonstrate practical or operational tasks for a helicopter during low-altitude flight. The data sets represent various levels of difficulty for range estimation algorithms. Each data set consists of 90 images and the associated supporting data described in the previous section. The first and last images of each data set are shown in figures 4-7. White dots in the figures indicate obstacles whose position has been measured. Since the laser tracker and most obstacles of interest are permanently fixed in position, a greater quantity of obstacle position information may be available in the future.

Line Data Set

The Line data set was acquired as the CH-47 flew a straight-line path between two rows of vehicles stationed along a runway. This data set demonstrates the deviation from theoretical straight-line motion that may be encountered under operational conditions for helicopter flight. The Line data set was designed to be simple both in terms of camera motion and scenery, and is therefore well suited for testing range estimation algorithms using flight data. The camera velocity is roughly 30 ft/sec along the optical axis, giving a camera motion of about 1 ft between successive images. Velocity components orthogonal to the optical axis change as much as 1.5 ft/sec over the 3-second period. Angular rates up to 0.05 rad/sec and changes in orientation of 0.03 rad are observed. The location of the lower-front and upper-rear corners on the right hand side of each obstacle was measured to provide true range information as well as data on the size of the obstacles. Range to the obstacles varies from 200 to 800 ft. The truck on the far right of figure 4 has an extensible 20 ft tower whose location was also determined.

Arc Data Set

The Arc data set uses the same simplified scenery as in the Line data set, but complexity of the camera motion is increased by having the helicopter follow an S-shaped ground path. The Arc data set captures one curve from that flight profile. The Arc sequence allows testing with simplified imagery of range estimation algorithms designed to operate with generalized camera motion. Peak angular velocity in yaw is about 0.13 rad/sec and is maintained for 1 sec. A bank angle of 0.045 rad is attained during the turn. Velocity along the camera's optical axis is roughly 40 ft/sec. The obstacles are 200 to 650 ft from the camera.

Posts Data Set

The Posts data set demonstrates straight-line motion but with imagery which contains both manmade and natural objects. The availability of distinct objects in the imagery (for example, the white posts) facilitates the validation of range estimates. The camera has a velocity of roughly 40 ft/sec along the optical axis. Distinctive objects are between 80 and 350 ft from the camera.

Towers Data Set

The Towers data set combines straight-line motion with very challenging imagery. An effective operational range estimation system should be able to successfully process data of this nature. The camera is moving at a velocity of 90 ft/sec along its optical axis. The nearest transmission towers are at a range of at least 450 ft.

SUMMARY AND CONCLUSIONS

A database has been developed based on a helicopter flight test experiment to allow validation of passive range estimation algorithms with realistic camera motion and visual scenery. The database includes video imagery, measurements of camera motion, and information on the characteristic parameters of the camera. In addition, independent measurements of range are included to allow verification of range estimates.

Four data sets from the larger database have been presented here. These data sets represent various camera motions and visual scenery, and were selected to provide a sequence of increasingly challenging tests for passive range estimation algorithms. These data sets will be available to researchers in the computer vision community.

Future plans include the development of a database to support multicamera methods of passive range estimation. Additional efforts may include the collection of infrared imagery to investigate the feasibility of performing range estimation at night.

APPENDIX

A few remarks concerning the image header data are in order to facilitate use of the data sets. It is noted that the image and header data for each sample time are provided in a single file stored in a HIPS-compatible format. A subroutine (written in the C programming language) which can access the image and header information will be provided with the data sets. Specific comments on the use of the header data follow.

Coordinate Systems

The coordinate systems used to express measurements contained in the data sets are illustrated in figure 2 and are defined below:

1. Earth (world) frame – The Earth frame (also called the world frame in the image headers) is rigidly affixed to the Earth with the X_e axis pointing North, the Y_e axis pointing East, and the Z_e axis pointing toward the center of the Earth. The origin of the Earth frame is an arbitrarily selected point on a runway at the test flight facility.

2. Helicopter body frame – The helicopter body axes frame (or body frame) is assumed to be fixed relative to the helicopter with the X_b axis pointing forward out the helicopter nose, the Y_b axis pointing out the right hand side of the helicopter, and the Z_b axis pointing downward relative to the helicopter's geometry (i.e., not necessarily toward the center of the Earth). The origin of the body frame is the helicopter's nominal center of gravity.

3. Image Plane Axes – The image plane axes are oriented along the rows and columns of the sensor array. The u axis points to the right along rows and the v axis points downward along the columns. The image plane axes originate at the image center (i.e., where the optical axis passes through the image plane).

4. Camera (sensor) frame – The camera frame is rigidly attached to the camera and originates at the lens focal point. The Y_s and Z_s axes are parallel to the image plane axes u and v, respectively. The X_s axis points along the optical axis. Since the camera is rigidly mounted to the helicopter, the location and orientation of the camera frame remains constant in body axes.

5. Pixel axes – The pixel axes, n_u and n_v, are attached to the camera's image plane and point along the rows and columns of the sensor array as do the image plane axes; however, the pixel axes originate at the upper left-hand corner of the sensor array rather than at the image center. In addition, distances along these axes are expressed in units of pixels (which are not necessarily square), so the coordinates of any point are its row and column indices in the image array. The upper left-hand pixel has coordinates (0,0).

Naming Convention

The naming convention for motion variables contained in the image headers is defined below:

1. Position, velocity, and angular rate measurements:
   a. The first term names a coordinate frame whose motion is to be given (i.e., SENSOR or BODY).

b. The second term indicates a motion state (i.e., POSITION, VELOCITY, or ANGULAR_RATE).

c. The final term specifies a component of the motion state (i.e., X_WORLD, Y_BODY, Z_SENSOR, etc.).

Example: SENSOR_POSITION_X_WORLD

Interpretation: component of sensor position along the X_e axis

2. Angle measurements:

a. The first term is always ANGLE.

b. The second term indicates the Euler angle to be specified (i.e., PSI, THETA, or PHI). See the following section, Rotation Matrices, for definition of the Euler angles.

c. The final term indicates the base coordinate frame and the destination coordinate frame (i.e., WORLD_TO_BODY, BODY_TO_SENSOR, WORLD_TO_SENSOR).

Example: ANGLE_PHI_WORLD_TO_BODY

Interpretation: bank angle of the body frame relative to the world frame

Rotation Matrices

The rotation matrices are defined in terms of Euler angles. The Euler angles are heading angle ψ, attitude angle θ, and bank angle ϕ. The rotation sequence is ψ about Z, θ about Y, and ϕ about X, where all rotations are positive in the right-hand sense. The rotation matrix resulting from this sequence of rotations is given below

$$R(\psi,\theta,\phi) = \begin{bmatrix} c\psi c\theta & s\psi c\theta & -s\theta \\ c\psi s\theta s\phi - s\psi c\phi & s\psi s\theta s\phi + c\psi c\phi & c\theta s\phi \\ c\psi s\theta c\phi + s\psi s\phi & s\psi s\theta c\phi - c\psi s\phi & c\theta c\phi \end{bmatrix}$$

The rotation matrix premultiplies a column vector to express that vector in another coordinate frame. The rotation matrices from the Earth frame to the body frame, from the body frame to the camera frame, and from the Earth frame to the camera frame are given by the following equations

$$R_{be} = R(\psi_{be}, \theta_{be}, \phi_{be})$$
$$R_{sb} = R(\psi_{sb}, \theta_{sb}, \phi_{sb})$$
$$R_{se} = R_{sb}R_{be} = R(\psi_{se}, \theta_{se}, \phi_{se})$$

where R_{be} is the rotation matrix from the Earth frame to the body frame, ψ_{be} is ANGLE_PSI_WORLD _TO_BODY, etc. The Euler angles are given in the image headers.

Perspective Projection Equations

The pixels which compose the images are not square for reasons discussed in reference 11. The pixel aspect ratio is defined as follows

$$b = \delta v / \delta u$$

where δu and δv are the horizontal and vertical pixel spacing, respectively. The effective focal length of the lens, f_e, is expressed in units of vertical pixels. The origin of the image plane coordinates (i.e., the image center) is located at (n_{u_0}, n_{v_0}) in the pixel axes system. With these definitions, the perspective projection equations which map points from the camera axes system to a pixel location in the image array are

$$n_u = n_{u_0} + bf_e(y_s/x_s)$$
$$n_v = n_{v_0} + f_e(z_s/x_s)$$

where (x_s, y_s, z_s) is the location of a point in camera axes and (n_u, n_v) is its projected location on the image plane in pixel axes. The following values are provided in the image header: b (ASPECT_RATIO), f_e (FOCAL_LENGTH), n_{u_0} (U_CENTER), and n_{v_0} (V_CENTER). The value of the vertical pixel spacing, δv, is 3.89×10^{-4} inch.

REFERENCES

1. Cheng, V. H. L.; and Sridhar, B.: Considerations for Automated Nap-of-the-Earth Rotorcraft Flight. Proceedings of the 1988 American Control Conference, Atlanta, Ga., June 15-17, 1988.

2. Sridhar, B.; Suorsa, R.; and Hussien, B.: Passive Range Estimation for Rotorcraft Low-altitude Flight. NASA TM-103897, October 1990.

3. Menon, P. K. A.; and Sridhar, B.: Passive Navigation Using Image Irradiance Tracking. AIAA Guidance, Navigation, and Control Conference, Boston, Mass., August 1989.

4. Barniv, Y.: Velocity Filtering Applied to Optical Flow Calculations. NASA TM-102802, August 1990.

5. Cheng, V. H. L.: Integration of Active and Passive Sensors for Obstacle Avoidance: IEEE Control Systems Magazine, vol. 10, no. 4, pp. 43-50, June 1990; also, Proceedings of the 1989 American Control Conference, Pittsburgh, Penn., June 1989.

6. Suorsa, R.; and Sridhar, B.: Validation of Vision Based Obstacle Detection Algorithms for Low Altitude Flight. Proceedings of the SPIE International Symposium on Advances in Intelligent Systems, Boston, Mass., November 1990.

7. Dutta, R.; Manmatha, R.; Williams, L. R.; and Riseman, E. M.: A Data Set for Quantitative Motion Analysis. Proceedings of the IEEE Computer Vision and Pattern Recognition Conference, pp. 159-164, San Diego, Calif., June 1989. Final Report, Pasadena, Calif., June 8-9, 1988.

8. Roberts, B.; and Bhanu, B.: Inertial Navigation Sensor Integrated Motion Analysis for Autonomous Vehicle Navigation. Proceedings of the DARPA Image Understanding Workshop, pp. 364-375, Pittsburgh, Penn., September 1990.

9. Thorpe, C.; and Kanade, T.: Carnagie Mellon Navlab Vision. Proceedings of the DARPA Image Understanding Workshop, Palo Alto, Calif., May 1989.

10. Bach, R. E., Jr.; and Wingrove, R. C.: Applications of State Estimation Applications in Aircraft Flight-Data Analysis. Journal of Aircraft, vol. 22, no. 7, pp. 547-554, July 1985.

11. Smith, P. N.: Flight Data Acquisition for Validation of Passive Ranging Algorithms for Obstacle Avoidance. NASA TM-102809, October 1990.

REPORT DOCUMENTATION PAGE

Form Approved
OMB No. 0704-0188

1. AGENCY USE ONLY *(Leave blank)*	2. REPORT DATE	3. REPORT TYPE AND DATES COVERED
	April 1992	Technical Memorandum

4. TITLE AND SUBTITLE

A Rotorcraft Flight Database for Validation of Vision-Based Ranging Algorithms

5. FUNDING NUMBERS

505-64-36

6. AUTHOR(S)

Phillip N. Smith

7. PERFORMING ORGANIZATION NAME(S) AND ADDRESS(ES)

Ames Research Center
Moffett Field, CA 94035-1000

8. PERFORMING ORGANIZATION REPORT NUMBER

A-92021

9. SPONSORING/MONITORING AGENCY NAME(S) AND ADDRESS(ES)

National Aeronautics and Space Administration
Washington, DC 20546-0001

10. SPONSORING/MONITORING AGENCY REPORT NUMBER

NASA TM-103906

11. SUPPLEMENTARY NOTES

Point of Contact: Phillip N. Smith, Ames Research Center, MS 210-9, Moffett Field, CA 94035-1000; (415) 604-5469 or FTS 464-5469

12a. DISTRIBUTION/AVAILABILITY STATEMENT

Unclassified — Unlimited
Subject Category 04

12b. DISTRIBUTION CODE

13. ABSTRACT ***(Maximum 200 words)***

Computer vision research has led to the development of several algorithms for estimating range to obstacles during low-altitude flight. However, due to the limited availability of "real world" data, algorithm verification has not been effectively addressed. A helicopter flight test experiment has been conducted at NASA Ames Research Center to obtain a database consisting of video imagery and accurate measurements of camera motion, camera calibration parameters, and true range information. The database was developed to allow verification of monocular passive range estimation algorithms for use in the autonomous navigation of rotorcraft during low altitude flight. This paper briefly describes the helicopter flight experiment and presents four data sets representative of the different helicopter maneuvers and the visual scenery encountered during the flight test. These data sets will be made available to researchers in the computer vision community.

14. SUBJECT TERMS	15. NUMBER OF PAGES
Passive range estimation, Helicopter test flight, Computer vision	15
	16. PRICE CODE: A02

17. SECURITY CLASSIFICATION OF REPORT	18. SECURITY CLASSIFICATION OF THIS PAGE	19. SECURITY CLASSIFICATION OF ABSTRACT	20. LIMITATION OF ABSTRACT
Unclassified	Unclassified		